The 8th International Conference on Jets, Wakes and Separated Flows, ICJWSF-2024
September 23-25, 2024, Firenze, Italy

Control of hydrogen jet mixing through use of coaxial air jet

N.M. Östman[1*], I.A.S. Larsson[1], D. Marjavaara[2] and F. Normann[2]

1: Division of Fluid and Experimental Mechanics, Luleå University of Technology, Sweden
2: LKAB, Kiruna, Sweden

[*] Corresponding author: martin.ostman@ltu.se

Abstract

In the process of indurating iron ore pellets, current grate-kiln plants use a coal-fired flame inside a rotary kiln, which results in the formation of CO_2 emissions. One alternative is to exchange coal for hydrogen as a fuel to reduce these emissions. In doing so, the mixing characteristics of fuel and secondary process air necessary for the combustion changes. To control the mixing, a coaxial jet can be used. The hydrogen fuel is injected through a central jet, surrounded by an annular jet from which air emanates. The aim is to investigate the effect of the momentum flow ratio between the outer and inner jet, M_{jet}, on the mixing. Steady-state simulations are performed in Ansys Fluent using a Reynolds-Stress turbulence model. Results show that changing M_{jet} offers the possibility to control the mixing of the hydrogen jet with the secondary air, thus affecting the length and spread of the jet.

Keyword: *CFD, coaxial jet, mixing, hydrogen jet*

1. Introduction

When producing iron ore pellets carbon dioxide emissions are generated at various stages of the process as fossil fuels are burned. During induration, the pellets are in current grate-kiln plants fired by a coal flame inside a rotary kiln. There is a desire to reduce the emissions from this process for environmental reasons.

Hydrogen can be used as an alternative fuel, but due its gaseous properties its mixing with the secondary process air differs from that of the solid coal [6]. The mixing is faster, which produces a shorter flame, something that is not suitable for the current application since the heat profile in the rotary kiln directly affects the quality of the pellets [8]. Other techniques of injecting the fuel therefore need to be evaluated. One possible solution is to use a so-called ‘coaxial jet’, or ‘co-jet’.

A co-jet consists of a central jet surrounded by an annular jet, through which two different fluids can be issued. The idea behind a co-jet solution is to use the annular jet fluid as a buffer between the secondary air and the central fuel jet. This can help slow down mixing of fuel and secondary air, and thus lengthen the resulting jet [5, 7]. The aim of this is to obtain a jet, and flame, that is similar to the reference coal flame.

In this study the parameter used to alter the behavior of the co-jet is the so-called ‘momentum flow ratio’, M_{jet}. It is defined as

$$M_{jet} = \frac{\rho_o u_o^2 A_o}{\rho_i u_i^2 A_i}, \tag{1}$$

where ρ is jet fluid density, u is jet exit velocity, and A is the jet exit cross-section area. Subscripts o and i in Eq. (1) stand for the outer and inner jet, respectively. By changing these parameters M_{jet} can be tuned to achieve the desired results. A case similar to that studied herein has previously been investigated [7], however in that case hydrogen was issued through both the inner and outer jet. Here it is instead of interest to examine the case where the fluid issued through the annular jet is different from the central jet. More specifically, air is used as the annular fluid.

The present work seeks to evaluate how the momentum flow ratio of a coaxial jet affects the mixing with a surrounding, co-flowing fluid. Computational Fluid Dynamics (CFD) simulations are used to simulate a simplified model of a rotary kiln. Length and spread of the hydrogen jet are used to quantify the results.

2. Method

2.1. Geometry and grid

The current study considers a simplified, axisymmetric, model of a full-scale rotary kiln. It is modeled as a constant diameter cylinder, with an annular inlet used to introduce the secondary process air. At the place where the secondary air inlet connects to the rotary kiln a wall is formed, called the 'back plate'. In the center of the back plate the coaxial jet is mounted. This simplified model allows for 2D axisymmetric CFD simulations to be carried out. The height of the back plate is one-third of the total kiln diameter, the remaining two-thirds are occupied by the secondary air inlet.

Figure 1a shows a sketch of the geometry considered in this study. The rotary kiln has a diameter $D = 5.04$ m, and length $L = 30$ m measured from the back plate. The secondary air inlet length is set to 10 m before it connects to the rotary kiln. In Fig. 1b the cross-section of the kiln, viewed from the outlet, is depicted as if it has been rotated around its axis of rotation. The division of secondary air inlet and back plate is seen.

In the CFD simulations a hexahedral grid is used, constructed using Ansys Meshing. The mesh consists of 210k elements, with refinements close to the jet inlet and the back plate to capture the shear layers that are formed. The mesh is shown in Fig. 2. By using a 2D model of the kiln, as opposed to a full 3D model, the mesh size and computational effort can be reduced. The simplification does come with some limitations, however they are here deemed acceptable. This is since the purpose of the study is to discover trends of changing the momentum flow ratio, and deepen the understanding of the mixing taking place.

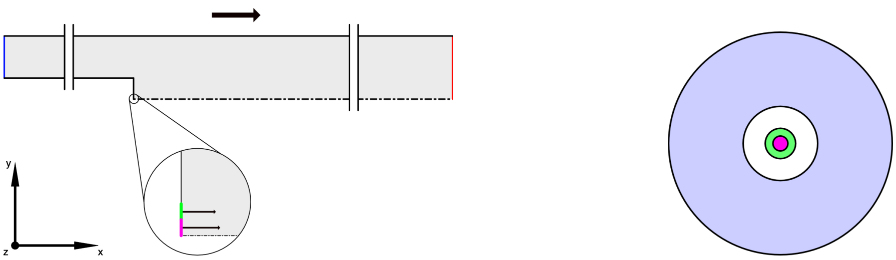

(a) (b)

Fig. 1: Geometry used in simulations; (a) 2D axisymmetric section, dashed line shows axis of rotation. Flow direction is from left to right, as indicated by the black arrow. (b) Model kiln viewed from the outlet, as if it had been rotated around its axis of rotation. Blue indicates inlet of secondary air, red is the outlet, green shows the outer jet and pink the inner jet. The white region between outer jet and secondary air inlet represents the back plate

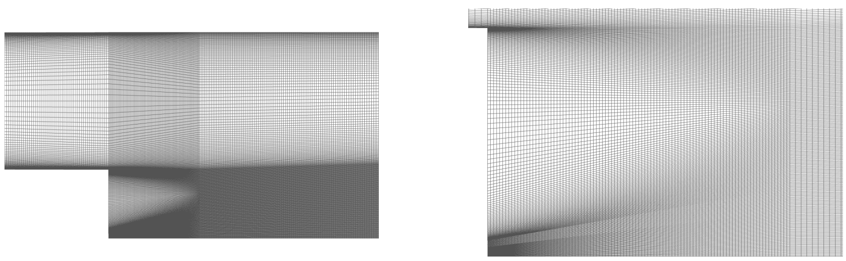

(a) (b)

Fig. 2: Numerical grid: (a) around the back plate, (b) area close to the jet

2.2. CFD simulations

CFD simulations were performed using the commercial software Ansys Fluent 2023 R1. The Reynolds Averaged Navier-Stokes (RANS) equations were closed by the Reynolds-Stress Baseline model (RSM-BSL). This model captures curvature in the flow more accurate than simpler eddy-viscosity models, such as $k - \omega$

SST [4, 1]. This ability is important since the jet is issued into a wake formed by the secondary air flowing past the bluff-body-like back plate, and this wake is known to have an effect on the resulting jet and flow field [3, 6].

All inlets are specified as mass flow inlets. The secondary air has density $\rho_{sec} = 0.245$ kg/m^3 and mass flow rate $\dot{m}_{sec} = 76.4$ kg/s, at 1473 K, based on the real process. The inner hydrogen jet has density $\rho_{H_2} = 0.0819$ kg/m^3 and mass flow rate $\dot{m}_{H_2} = 0.28$ kg/s, at 300 K. The mass flow of hydrogen is set to match the kinetic energy and power of the coal jet used in the current rotary kiln. Finally, the outer air jet is specified as air at 330 K with density $\rho_{airjet} = 1.067$ kg/m^3, and varied mass flow rate $\dot{m}_{airjet}$.

Equations for pressure and momentum are discretized using a second-order scheme, while turbulence quantities use a first-order upwind scheme. Iteration of the solution is performed using a pseudo time step method. All simulations use double precision.

2.3. Co-jet configurations

Five values of the momentum flow ratio, Eq. (1), are evaluated: $M_{jet} = [0.25,\ 0.5,\ 0.75,\ 1,\ 2]$. The aim of the study is to investigate how this ratio can be used to tweak the length and mixing of the hydrogen jet. The value of M_{jet} is changed by using different velocities through the outer jet, achieved by altering the mass flow rate of air and keeping the jet radius constant. For all cases the central hydrogen jet remains unchanged. Table 1 shows the parameters used to achieve each case. In addition, the case without an annular jet is shown for comparison.

Tab. 1: Parameter values used in simulations of coaxial jets

M_{jet} [−]	$\dot{m}_o$ [kg/s]	$\dot{m}_i$ [kg/s]	u_o [m/s]	u_i [m/s]
Single jet	–	0.28	–	472
0.25	0.86	0.28	38	472
0.5	1.22	0.28	54	472
0.75	1.50	0.28	67	472
1	1.73	0.28	77	472
2	2.46	0.28	109	472

2.4. Grid study

A grid study was performed, using Richardson extrapolation on three grids, to establish the numerical accuracy of the simulations [2]. To compare different grids, the dimensionless jet length L_{jet} and pressure ratio P_{in}/P_{out} were used as dependent variables. Table 2 shows the results of the study. The extrapolated and approximate relative error, along with the fine-grid convergence index, are shown. Due to the small errors between grids, the one consisting of 210k elements was used in the simulations. This mesh produced y^+-values in the range $0.34 - 57$, however the larger values are assumed to not influence the main results shown herein. This is since the chosen solver uses a y^+-insensitive wall formulation, that employs a wall-function approach when the mesh resolution is too poor, as opposed to fully resolving the viscous sublayer [1]. Further, this study mainly looks at the flow away from solid boundaries.

Tab. 2: Results of the grid study

Grid number	Element count	P_{in}/P_{out}	L_{jet}
3	118k	1.0599	0.1801
2	210k	1.0659	0.1749
1	328k	1.0684	0.1736
Extrapolated	∞	1.0719	0.1728
e^{21}_{ext}		0.3%	0.5%
e^{21}_{a}		0.2%	0.8%
GCI^{21}_{fine}		0.4%	0.6%

3. Results

In what follows the results from the CFD simulations are presented. The overall flow field close to the jet and back plate is shown, along with contours of hydrogen concentration. Profiles of velocity and hydrogen concentration are shown along the kiln centerline and at cross-sections. Finally, jet mixing is quantified using entrainment. Velocities have been scaled by the velocity of the inner hydrogen jet. Plots of hydrogen concentration are scaled by the concentration at the hydrogen jet inlet.

3.1. Flow field

Figure 3 shows contours of axial velocity in an area close to the jet, with streamlines to visualize the flow field, for a coaxial jet with $M_{jet} = 1$. The contours are mirrored along the rotational axis $y = 0$. As seen, the flow field consists largely of a recirculation zone. This is formed as the secondary air flows over the back plate, which acts as a bluff body.

The hydrogen concentration contours in Fig. 4 show how the jet evolution is affected as the coaxial jet is introduced. Further, the effect of changing M_{jet} is seen. It can be observed that higher values of M_{jet} produce a narrower jet for $x/D < 1$. Table 3 displays the jet length and wake length that result from using the different co-jet configurations. As seen, a higher value of M_{jet} gives a longer jet.

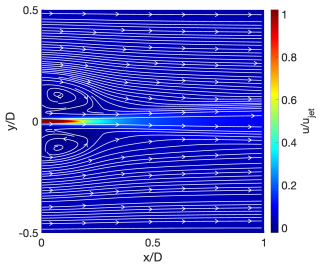

Fig. 3: Flow field colored by axial velocity for a co-jet having $M_{jet} = 1$

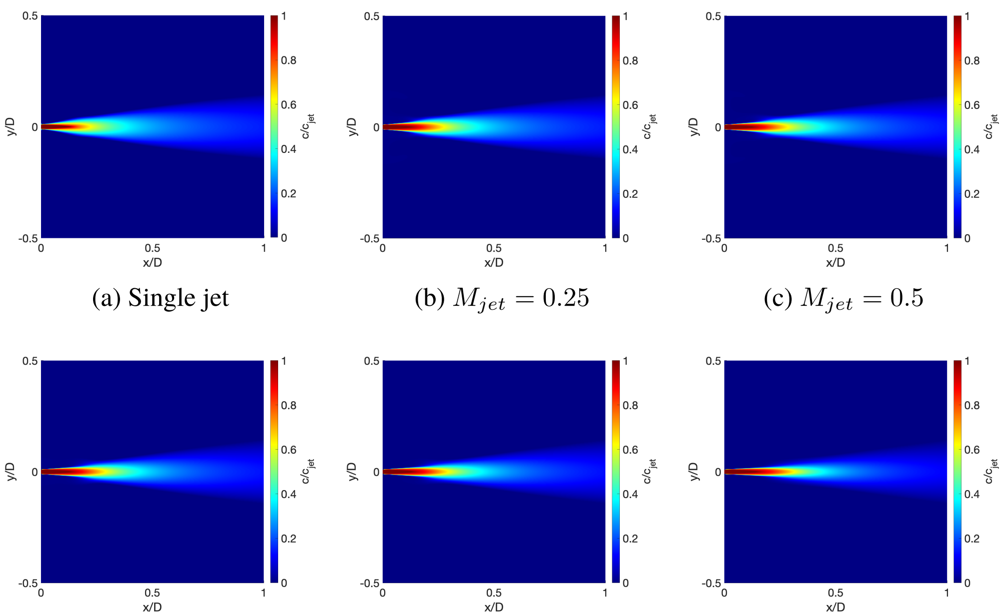

(a) Single jet (b) $M_{jet} = 0.25$ (c) $M_{jet} = 0.5$

(d) $M_{jet} = 0.75$ (e) $M_{jet} = 1$ (f) $M_{jet} = 2$

Fig. 4: Contours of hydrogen concentration for (a) a single hydrogen jet, and (b–f) different values of M_{jet}

3.2. Axial profiles

Figure 5 shows velocity and hydrogen concentration at cross-sections along the length of the rotary kiln. In the figure, the different co-jet configurations are compared to the case with a single hydrogen jet. What can be seen is that the length of the jet is increased as M_{jet} is increased. The difference is more prominent

Tab. 3: Jet length and wake length for different values of M_{jet}, and for a single hydrogen jet

M_{jet}	Dimensionless jet length	Dimensionless wake length
Single jet	0.14	0.23
0.25	0.16	0.26
0.5	0.17	0.27
0.75	0.17	0.26
1	0.17	0.25
2	0.19	0.23

closer to the jet exit. It is also clear that the introduction of the outer air jet has an effect on the jet evolution that takes place between the two locations.

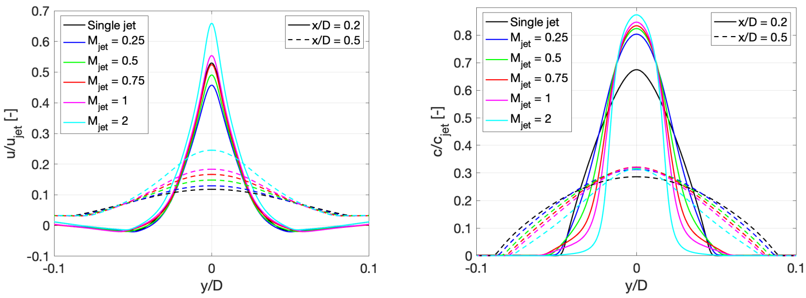

(a) Axial velocity (b) Hydrogen concentration

Fig. 5: Axial profiles of velocity and hydrogen concentration

3.3. Jet entrainment

How much the hydrogen jet has spread can be determined using the concept of entrainment. It tells how much of the surrounding secondary air, and outer air jet, has been incorporated, or entrained, into the hydrogen jet. There are various measures to use when investigating this, two of which are used herein. These are the jet half-width $r_{1/2}$ and the entrainment coefficient Q/Q_0. The jet half-width is the distance from the jet centerline to the radial point at which the concentration of hydrogen has decreased to 50% of its value at the centerline. The entrainment coefficient is the ratio between the volumetric flow rate Q inside the jet boundary (defined by the jet half-width), and the volumetric flow rate entering through the jet nozzle, Q_0. It then tells how much the volumetric flow rate of the jet has increased due to entrainment.

Figure 6 shows plots of the jet half-width and the entrainment coefficient. As seen, the cases in which an outer air jet is used initially provide a more confined jet with less entrainment (Figs.6a and 6c). More specifically, a higher value of M_{jet} delays the jet spread (Fig. 6a). Further downstream (Figs. 6b and 6d), however, the coaxial jet cases actually show more spread than the single hydrogen jet. The reason for this is possibly that the higher velocity of the outer jet promotes entrainment of secondary air, due to increased shear with the secondary air.

4. Conclusions

A coaxial jet consisting of a central hydrogen jet and an annular air jet, issued into co-flowing surrounding air, has been studied using CFD. The momentum flow ratio M_{jet} of the coaxial jet has been altered, and its effect on the flow field and mixing has been evaluated. From the findings presented in this study it is concluded that by introducing an annular air jet around the hydrogen jet, the jet core length is extended. Further, by altering the value of M_{jet} the jet length can be tweaked. This is since the air jet acts as a buffer around the central hydrogen jet, protecting it from being mixed with the secondary air through shear.

Increasing the value of M_{jet} lengthens the inner jet core. This is achieved by increasing the velocity, and thus momentum, of the outer air jet. This allows the outer jet to penetrate further into the rotary kiln and act as a protective layer for the inner jet over a greater distance. Plots of velocity and hydrogen concentration show these trends.

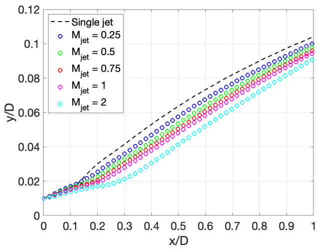

(a) Concentration half-width close to the jet

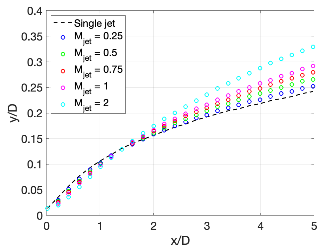

(b) Concentration half-width downstream

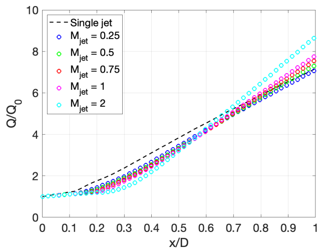

(c) Entrainment coefficient close to the jet

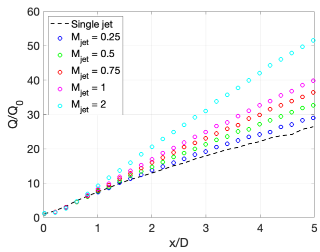

(d) Entrainment coefficient downstream

Fig. 6: Plots of (a–b) concentration half-width and (c–d) entrainment coefficient, close to the jet and further downstream

Plots of the jet half-width and entrainment coefficient suggest that increasing the value of M_{jet} narrows the jet close to the jet exit. Further downstream, however, the situation is switched and higher values of the momentum flow ratio show faster jet spread and more entrainment of ambient fluid.

Results show that more simulations, possibly under more realistic circumstances and using an extended range of parameter values, need to be carried out to gain further insights into the dynamics of the flow and mixing taking place. In addition, experiments can be performed to validate the numerical results.

References

[1] ANSYS, Inc. *Ansys Fluent Theory Guide, Release 2023 R1*. 2023.

[2] I. Celik et al. “Procedure for Estimation and Reporting of Uncertainty Due to Discretization in CFD Applications”. In: *Journal of Fluids Engineering* 130.7 (July 2008), p. 078001. ISSN: 0098-2202. DOI: 10.1115/1.2960953. URL: https://doi.org/10.1115/1.2960953.

[3] S M Correa and A Gulati. “Measurements and Modeling of a Bluff Body Stabilized Flame”. In: *Combustion and Flame* 89.2 (1992), pp. 195–213. DOI: 10.1016/0010-2180(92)90028-N.

[4] I. A. Sofia Larsson, T. Staffan Lundström, and B. Daniel Marjavaara. “Calculation of kiln aerodynamics with two RANS turbulence models and by DDES”. In: *Flow, Turbulence and Combustion* 94.4 (June 2015), pp. 859–878. ISSN: 15731987. DOI: 10.1007/s10494-015-9602-8.

[5] I. A. Sofia Larsson et al. “Experimental study of confined coaxial jets in a non-axisymmetric co-flow”. In: *Experiments in Fluids* 61.12 (Dec. 2020). ISSN: 14321114. DOI: 10.1007/s00348-020-03094-3.

[6] Peter Mullinger and Barrie Jenkins. *Industrial and Process Furnaces. Principles, Design and Operation*. Third edition. Butterworth-Heinemann, 2023. ISBN: 9780323916295.

[7] N. Martin Östman et al. “Effect of momentum flow ratio on entrainment of a confined coaxial jet in a co-flow”. In: *Engineering Applications of Computational Fluid Mechanics* 18.1 (June 2024), p. 2374977. ISSN: 1997003X. DOI: 10.1080/19942060.2024.2374977.

[8] Henrik Wiinikka et al. “Combustion Evaluation of Renewable Fuels for Iron-Ore Pellet Induration”. In: *Energy and Fuels* 33.8 (Aug. 2019), pp. 7819–7829. ISSN: 15205029. DOI: 10.1021/acs.energyfuels.9b01356.